Published in final edited form as:
Free Radic Biol Med. 2012 November 15; 53(10): 1968–1976. doi:10.1016/j.freeradbiomed.2012.08.013.

Glutathiyl Radical as an Intermediate in the Glutathione Nitrosation*

Kumpal Madrasi[1], **Mahesh S. Joshi**[1,a], **Tushar Gadkari**[1], **Konstantinos Kavallieratos**[2], and **Nikolaos M. Tsoukias**[1]

[1]Department of Biomedical Engineering, Florida International University, Miami, FL 33174

[2]Department of Chemistry and Biochemistry, Florida International University, Miami, FL 33199

Abstract

Nitrosation of thiols is thought to be mediated by Dinitrogen Trioxide (N_2O_3) or by Nitrogen Dioxide radical ($^{\bullet}NO_2$). A kinetic study of Glutathione (GSH) nitrosation by NO donors in aerated buffered solutions was undertaken. S-nitrosoglutathione (GSNO) formation was assessed spectrophotometrically and by chemiluminescence. Results suggest an increase in the rate of GSNO formation with an increase in GSH with a half-maximum constant EC_{50} that depends on NO concentration. Our observed increase in EC_{50} with NO concentration suggests a significant contribution of $^{\bullet}NO_2$ mediated nitrosation with the glutathiyl radical as an intermediate in the production of GSNO.

Keywords

Glutathione; nitric oxide; thiyl radical; kinetics

Introduction

Blood vessel dilation [1], signal conduction in nervous system [2], and cytotoxic activity against microbes [3] are amongst the important physiological roles played by NO. For free NO to perform these functions, it should be able to reach its sites of action without being scavenged through its reaction with heme proteins[4]. Formation of nitrosothiols can increase the half – life of NO in the vasculature and thus can enhance its biological functions. The formation of β–93 cysteine nitrosothiols on the hemoglobin molecule [5]and the combination of NO with low molecular weight thiols are two candidate pathways for NO preservation[6]. Nitrosothiols have been found to be potent vasodilators and inhibitors of platelet aggregation and may also play important roles in signaling pathways. In view of the importance of nitrosothiols in biological systems, it is of interest to elucidate the kinetic mechanism and assess the rate of their formation. Of particular interest is the nitrosation of glutathione due to its abundance in biological tissues [38]. Glutathione nitrosation has been proposed to occur via an initial reaction of NO with O_2 and the subsequent formation of

[a]Correspondence to: Mahesh S. Joshi, Ph.D. Department of Biomedical Engineering, 10555 W. Flagler Street, Florida International University, Miami, FL 33174. Tel: 305-348-7292. Fax: 305-348-6954. mjoshi@fiu.edu.

N_2O_3, which acts as the nitrosating agent for GSH. The suggested reaction mechanism for this route of nitrosation is as follows [7,17, 33, 36]:

$$2NO+O_2 \xrightarrow{k_1} 2NO_2 \quad \text{Reaction 1}$$

$$NO_2+NO \underset{k_{-2}}{\overset{k_2}{\rightleftharpoons}} N_2O_3 \quad \text{Reaction 2}$$

$$GSH+N_2O_3 \xrightarrow{k_3} GSNO+NO_2^-+H^+ \quad \text{Reaction 3}$$

$$N_2O_3+H_2O \xrightarrow{k_4} 2NO_2^-+2H^+ \quad \text{Reaction 4}$$

Recent evidence shows that in adequately oxygenated solutions the $^{\bullet}NO_2$ can oxidize the GSH to form the glutathiyl radical ($GS^{\bullet}$) which reacts with NO to form GSNO [8, 16, 22, 39]. This scheme would include the same rate limiting step (Reaction 1) as well as Reactions 2 and 4. However, nitrosation would proceed through Reactions 5 and 6 instead of 3.

$$^{\cdot}NO_2+GSH \xrightarrow{k_5} GS^{\cdot}+NO_2^- \quad \text{Reaction 5}$$

$$GS^{\cdot}+{}^{\cdot}NO \xrightarrow{k_6} GSNO \quad \text{Reaction 6}$$

Thus, according to the second kinetic mechanism the $^{\bullet}NO_2$ can react with GSH to give GSNO (Reaction 5), but also reacts with NO to form N_2O_3 (Reaction 2). This cross talk between the two alternative pathways poses a significant obstacle in determining the relative contribution of the two mechanisms. Thus, despite recent evidence that propose $^{\bullet}NO_2$ as the active intermediate for nitrosation [8, 16, 22, 39], the importance of N_2O_3 vs $^{\bullet}NO_2$ in thiol nitrosation has not been conclusively determined [7, 17, 33, 36]. In this study, we have followed the kinetics of the GSH nitrosation reaction in an attempt to elucidate the reaction mechanism and to identify the role of N_2O_3 and $^{\bullet}NO_2$ as nitrosating intermediates.

Recent data [22] has documented significant GSSG formation during the nitrosation of GSH by NO donors, which involves the formation of the thiyl radical. This essentially validates the second reaction mechanism above, since the presence of GSSG means that there has been formation of the glutathiyl radical ($GS^{\bullet}$). One potential route of GSSG formation is through the following series of reactions:

$$GSH \underset{k_{-7}}{\overset{k_7}{\rightleftharpoons}} GS^- + H^+ \quad \text{Reaction 7}$$

$$GS^{\cdot}+GS^- \underset{k_{-8}}{\overset{k_8}{\rightleftharpoons}} GSSG^- \quad \text{Reaction 8}$$

$$GSSG^-+O_2 \xrightarrow{k_9} GSSG+O_2^{\cdot-} \quad \text{Reaction 9}$$

Alternatively, GSSG can be formed from GSNO according to Reaction 10 [50].

$$GS^{\cdot} + GSNO \xrightarrow{k_{10}} GSSG + {}^{\cdot}NO \quad \text{Reaction 10}$$

The proposed, simplified kinetic mechanisms do not consider a number of relevant reactions including alternative reactions for GSSG formation as well other reactions that are involved in GSH and NO oxidation chemistry. In the Supplement, we present a mathematical model of 25 relevant reactions and we compare model predictions for GSNO formation rate against the output of the two simplified reaction schemes.

Materials and Methods

Materials

Glutathione (GSH), N-Ethyl Maleimide (NEM), and Diethylene Triamine Pentaacetic Acid (DTPA) were obtained from Sigma Aldrich Co (St. Louis, MO). NO donors Propylamine Propylamine NONOate and Diethylamine NONOate (PAPA/NO and DEA/NO) and S-nitrosoglutathione were obtained from Cayman Chemical Co (Ann Arbor, MI).

NO release by NO donor

NO donors were chosen with an appropriate half – life; a suitably long half – life confers on them the ability to generate steady NO levels over the duration of the experiment (see results section). At 20–25°C PAPA/NO and DEA/NO have a half – life of approximately 77 min and 16 min respectively. To validate theoretical predictions for the pattern of NO release from NO donors, we used different concentrations of PAPA/NO ranging from 500 μM to 10 mM in a pH of 7.4 and measured NO release using a commercially available NO-sensitive electrode (WPI, Sarasota, FL).

GSNO measurements

UV-visible spectro-photometry was carried out by a Cary 100 Bio UV-Vis spectrophotometer. GSH concentrations ranged from 200 μM to 5mM and PAPA/NO concentrations from 500 μM to 10 mM. Reactions were carried out in 1 mL size quartz cuvettes as in Fields et al. [9]. GSNO formation in a mixture of GSH and PAPA/NO was followed at 338 nm (molar absorptivity of 900 $M^{-1}cm^{-1}$) [10]. We also measured GSNO formed using chemiluminescence analysis. The Copper (I) Chloride and Cysteine (2C) assay method was used to measure GSNO through a chemiluminescence analyzer (Sievers 280i NOA) as described in earlier works [11,12,24, 73]. Different GSH concentrations (200 μM to 7.5 mM) and DEA/NO (31.25 μM to 500 μM) were incubated in Eppendorf tubes. Reactions were stopped with 10 mM NEM at 2, 3 and 4 minutes. The solutions were left at room temperature in the dark for about an hour for the NO donor to completely decay, so as to avoid any NO signal in the assay from the NO donor. Following this period, GSNO content in our samples was analyzed. All reactions followed by spectrophotometry or by chemiluminescence were performed in 40 mM phosphate buffer (pH = 7.4) supplemented by 50 μM DTPA at 20–25 °C. To check for interference from other NO-derived species, samples were incubated with 2.5 mM $HgCl_2$ for half an hour to abolish GSNO content [13] prior to the 2C assay.

“Clamped NO” protocol

A combination of an NO donor and an NO scavenger (i.e. CPTIO) has been previously utilized to maintain steady levels of NO in solution (i.e. “clamped NO protocol” [59]). We hypothesized that a similar “clamped NO” condition can be achieved in aerated solutions of NO donors where O_2 will be the predominant NO scavenger. Thus, a relative steady NO

concentration is expected as a result of the balance between NO release by the donor and consumption by the oxygen content of the solution. We also refer to this as the "clamped NO concentration" similar to Griffith et al.[59].

Assuming that every mole of NO donor releases n moles of NO, the NO release rate by the NO donor is given by Eq. 1a.

$$S = nk_d[\mathrm{NOdonor}]e^{-k_d t} \quad \text{Eq. (1a)}$$

where $k_d = \ln(2)/t_{1/2}$ and $t_{1/2}$ is the half – life of the NO donor. For times less than 1/10 of the half – life of the NO donor the release rate remains relatively constant and can be approximated by:

$$S = nk_d[\mathrm{NOdonor}] \quad \text{Eq. (1b)}$$

In the absence of other NO scavengers NO is consumed through the reaction with dissolved O_2 (Reaction 1) and through Reaction 2. Reaction 1 is the rate-limiting reaction and thus total NO consumption can be approximated by:

$$R = 4k_1[O_2][NO]^2 \quad \text{Eq. (1c)}$$

At equilibrium, the balance between Eq. 1b and Eq. 1c yields a steady NO level:

$$[NO] = \sqrt{\frac{nk_d}{4k_1[O_2]}}\sqrt{[\mathrm{NOdonor}]} \quad \text{Eq. (1d)}$$

Thus, NO levels should remain relatively constant and concentrations should increase proportionally to the square root of the NO donor concentration.

Pseudo steady state approximation

A pseudo steady state approximation has been previously employed by Kharitonov et al. to simplify the kinetic mechanism (Reactions 1–4) [17]. Assuming small concentration of unstable intermediates $^{\bullet}NO_2$, N_2O_3 and thus negligible rates of change for these complexes we get:

$$\frac{d[\mathrm{GSNO}]}{dt} = \frac{2k_1[NO]^2[O_2][\mathrm{GSH}]}{[\mathrm{GSH}] + \frac{k_4}{k_3}} \quad \text{Eq. (2a)}$$

On the other hand, the pseudo steady state approximation for the Reactions 1, 2, 4, 5, and 6 gives us the rate of nitrosation as:

$$\frac{d[\mathrm{GSNO}]}{dt} = \frac{2k_1[NO]^2[O_2][\mathrm{GSH}]}{[\mathrm{GSH}] + \frac{k_2k_4[NO]}{[k_{-2}+k_4]k_5}} \quad \text{Eq. (2b)}$$

Note that Eq. 2b in agreement with Eq. 2a suggests saturation kinetics with respect to the concentration of GSH. In Eq. 2b, however, the half-maximum constant EC_{50} is dependent on the NO concentration. Thus, an effective EC_{50} value equal to $\frac{k_2k_4[NO]}{[k_{-2}+k_4]k_5}$ is predicted.

Experimentation will test the saturation kinetics of this rate law. Thus the rate of GSNO formation will be equal to the product of the maximum rate at saturating concentrations ($V_{max} = 2k_1[NO]^2[O_2]$) times a factor *m* that differs between the two proposed mechanisms. According to the first mechanism (Eq. 2a), $m_1 = \frac{k_3[GSH]}{k_3[GSH]+k_4}$ while based on Eq. 2b, $m_2 = \frac{k_5[GSH]}{k_5[GSH]+\frac{k_2k_4[NO]}{(k_{-2}+k_4)}}$. Eq. 2a and 2b simply state that the rate is limited by the rate of NO oxidation (Reaction 1) and the fraction of N_2O_3 or $^{\bullet}NO_2$ utilized in GSH nitrosation ($m_1 = \frac{Rxn\ 3}{Rxn\ 3+Rxn\ 4}$, $m_2 = \frac{Rxn\ 5}{Rxn\ 5+Rxn\ 2}$). The functional difference between the two mechanisms arise from the NO dependency in the scavenging of the active intermediate in mechanism 2 (i.e. $^{\bullet}NO_2$ scavenging through Reaction 2) vs the NO-independent consumption of the active intermediate in mechanism 1 (i.e. N_2O_3 scavenging through Reaction 4). Based on Eq. 2b, EC_{50} will increase with NO concentration, if $^{\bullet}NO_2$ is the major nitrosating intermediate. On the other hand, based on Eq. 2a, an EC_{50} value that remains relative steady at different levels of NO, is indicative of N_2O_3 as the nitrosating intermediate.

When we incorporate Reactions 7–9 into kinetic mechanism 2 to account for the formation of GSSG, PSSA yields:

$$\frac{d[GSNO]}{dt} = \frac{2k_1[NO]^2[O_2][GSH]}{[GSH]+\frac{k_2k_4}{[k_{-2}+k_4]k_5}[NO]} \times \frac{k_6[NO]}{k_6[NO]+\frac{k_8k_7}{k_{-7}}[GSH]} \quad \text{Eq. (2c)}$$

The difference between Eq. 2c and 2b is a correction factor $f = \frac{k_6[NO]}{k_6[NO]+\frac{k_8k_7}{k_{-7}}[GSH]}$ that accounts for the fraction of total $GS^{\bullet}$ utilized in the formation of GSNO (i.e. $f = \frac{Rxn\ 6}{Rxn\ 6+Rxn\ 8}$). Eq. 2c reduces to Eq. 2b when $\frac{[NO]}{[GSH]} \gg \frac{k_8k_7}{k_6k_{-7}}$. Incorporating Reaction 7–10 to the simplified kinetic mechanism 2 and applying PSSA yields:

$$\frac{d[GSNO]}{dt} = \frac{2k_1[NO]^2[O_2][GSH]}{[GSH]+\frac{k_4k_2[NO]}{[k_{-2}+k_4]k_5}} \times \frac{k_6[NO]-k_{10}[GSNO]}{k_6[NO]+\frac{k_8k_7[GSH]}{k_{-7}}+k_{10}[GSNO]} \quad \text{Eq. (2d)}$$

For low GSNO levels (i.e. $[GSNO] \ll \frac{k_6}{k_{10}}[NO]$) Eq. 2d reduces to Eq 2c, thus Reaction 10 should not affect initial formation rates. However, Eq. 2d suggests that in a “clamped NO” condition, GSNO accumulation will lead to an equilibrium point with steady GSNO levels i.e. $[GSNO] = \frac{k_6}{k_{10}}[NO]$.

Results

Dependence of [NO] on [NO donor]

First, we investigated the pattern of NO release by NO donors to confirm our theoretical predictions (Eq. 1d). NO release was measured with varying concentrations of PAPA/NO (500 μM to 10 mM) electrochemically using an NO electrode. A sample reading is shown in Fig. 1A. As NO release occurs, concentration levels rise to a peak value before reaching a slowly decaying plateau. As expected, decay in NO concentration occurs as a result of NO donor consumption over time. The long half – life of the NO donor allows for a relative steady level of NO over an adequate time frame. Peak NO concentrations from NO recordings at different NO donor concentrations were used to generate a log − log graph of [NO] vs. [PAPA/NO] (n=4). The result is shown in Fig. 1B. The linear relationship between log[NO] and log[PAPA/NO] has a slope of 0.51 ± 0.04 and it is not statistically different

from 1/2(p =0.30). As expected, based on Eq. 1d, established NO levels are proportional to the square root of the utilized NO donor concentration, i.e. $[NO] \propto \sqrt{[NOdonor]}$.

Electrode data thus yield the following linear relationship between clamped [NO] and $\sqrt{[PAPA/NO]}$

$$[NO]=0.23 \pm 0.02 \sqrt{[PAPA/NO]} \quad \text{Eq. (3)}$$

This result would be in agreement with Eq. 1d for $n\times k_d = 1.58\pm0.03 \times 10^{-4} s^{-1}$ for PAPA/NO under the conditions of our experiment. [Reported stoichiometry (n=2) and half – life($t_{1/2}$= 77 minutes) [14, 15] for PAPA/NO at room temperature yield $n\times k_d = 3 \times 10^{-4}\ s^{-1}$ but these values may change with experimental conditions [60, 61]]. We use Eq. 3 to better predict [NO] for every [PAPA/NO] in further analysis rather than using Eq. 1d with the reported half – life of PAPA/NO.

Dependence of EC_{50} on [NO]

Fig. 2A shows a representative recording of GSNO formation in the spectrophotometer for a particular GSH (250 μM) and NO donor concentration (PAPA/NO; 1mM). Recordings show a relative constant rate of GSNO formation over a period of a few minutes. The slope of this tracing where NO concentration would have peaked was recorded (red circle in Fig. 2A) and corresponds to the maximum rate of GSH nitrosation at the particular NO donor and GSH concentration. The use of this slope rather than initial slope is necessitated to account for the time required for NO to evolve. We ensure that peak/plateau NO concentration is reached fast after mixing with GSH and thus GSH concentration has not changed significantly from initial time and formation of GSNO is low (i.e. $[GSNO] \ll \frac{k_6}{k_{10}}[NO]$). Experiments were repeated for different GSH concentrations at each NO donor concentration and the results are summarized in Fig. 2B for three PAPA/NO concentrations (500 μM, 1 mM and 5 mM). In the inset, V_{max}/V vs. 1/GSH plots were made ('V' indicates the rate of nitrosation). Linear least square fittings followed by taking the slope yields EC_{50} values at each NO donor concentration. We observe a NO concentration dependent shift in EC_{50} values. As the NO donor concentration increases the EC_{50} value also increases.

Fig. 3A depicts the dependence of the half maximum constant EC_{50} as a function of the NO donor concentration in a log − log plot. EC_{50} values are averaged over n ≥ 3 experiments. A liner fit of the dependence of log(EC_{50})vs. log (PAPA/NO) reveals a slope of 0.5± 0.2 which is not statistically different from 1/2(p = 0.946). The above data point towards an EC_{50} value proportional to the square root of the NO donor (PAPA/NO) i.e. $EC_{50} \propto \sqrt{[NOdonor]}$. Thus, experiments point towards an EC_{50} value that is linearly dependent on the square root of NO donor and as a result proportional to the clamped NO concentration, i.e. $EC_{50} \propto [NO]$.

NO donor concentrations were related to NO concentrations using experimental data from Fig. 1B. (Alternatively, one can use Eq. 1d if the stoichiometry and half – life of the NO donor is known). We then can plot EC_{50} values from Fig. 3A as a function of [NO] (Fig. 3B). A linear dependence is observed in Fig. 3B with a slope of 30.5 ± 5.2 μM GSH/μM NO.

$$EC_{50}=30.5\,[NO] \quad \text{Eq. (4)}$$

Experiments were repeated in a chemiluminescence analyzer following the 2C assay method from Gaston et al. [73] using different DEA/NO and GSH concentrations. This NO donor had a reasonably short half –life so as to allow both for a "clamped NO" condition (over a short period of time), and provide an early elimination of NO donor from the solution. The latter condition is needed to avoid interferences in the chemiluminescence device due to NO release by the donor when GSNO levels are measured. Recordings were collected for each GSH and NO donor concentration and were compared against a predetermined calibration curve prepared from known concentrations of GSNO(data not shown). Rates of GSNO formation were obtained by dividing GSNO concentrations by the corresponding incubation/reaction times. The control experiments where GSNO content was abolished with $HgCl_2$ showed zero signal, hence confirming that the signal obtained was from GSNO. The estimated GSNO production rates were used to calculate EC_{50} using curve fitting similar to Fig. 2B. A slope of 0.38 ± 0.07 in the log EC_{50} vs log [DEA/NO] data was estimated (n = 3). This is slightly different than the slope of approximately 0.5 from the earlier method. This may be attributed to some GSNO scavenging during the hour-long post reaction incubation time (see methods section). However, the alternative explanation for participation of N_2O_3 in nitrosation of GSH cannot be excluded.

Calculation of k_5

This constant applies to the overall reaction of $NO_2^{\cdot}$ with both the thiol and the thiolate anion and it is pH dependent[31] (See also table T1). Based on our analysis the dependence of EC_{50} on [NO] is linear with a slope that is equal to $\frac{k_4 k_2}{(k_{-2}+k_4)k_5}$. Then assuming the values for the other kinetic constants (k_2, k_{-2}, k_4) from Table 1 and a slope of 30.5 μM GSH/μM NO from Eq. 3 a value for k_5 of 1.15×10^7 $M^{-1}s^{-1}$ is predicted. This is essentially the same as the experimentally observed value by Ford et al. [31], (derived from Fig. 2 in [31] for pH = 7.4), and reasonably close to their corrected estimate of 2×10^7 $M^{-1}s^{-1}$ which takes account the reduction of $GS^{\bullet}$ at higher pH values in their analysis. The rate constant of N_2O_3 hydrolysis (Reaction 4) was determined from Eq. 9 and accounts for catalysis by 40mM of phosphate [18,44], i.e. $K_4 = (530 + K_P\,[Pi])$ where $k_p = 9.4\times10^5$ $M^{-1}s^{-1}$[18,44].

Dependence of V_{max} on [NO]

In Fig. 4A, we plot V_{max} against PAPA/NO concentrations in a log − log plot. A slope of 1.09 ± 0.1 in the log − log plot suggests a linear dependence between V_{max} and [PAPA/NO] (i.e. a square dependence on [NO] in agreement with both kinetic mechanisms). A linear plot of V_{max} vs [PAPA/NO] reveals a slope of (7.5 ± 0.5) $\times10^{-5}$ s^{-1}(Fig. 4B).

$$V_{max}=7.5\times10^{-5}[\mathrm{PAPA/NO}] \quad \text{Eq. (5a)}$$

Based on both kinetic mechanisms (Eq. 2a or 2b) $V_{max} = 2k_1[NO]^2[O_2]$. [Note: Eqs 2c & d predict different V_{max} dependence on NO and differences with Eq. 2b can become significant at high GSH or GSNO concentrations. However, experimental data and model simulations (see below) suggest that under our experimental conditions these differences are negligible].

Using Eq. 1d, and the previously determined value for $n\times k_d = 1.58 \pm 0.03 \times 10^{-4}s^{-1}$ from the electrode data, we predict that:

$$V_{max}=2k_1[NO]^2[O_2]=\frac{nk_d}{2}[\mathrm{NOdonor}]=7.9\times10^{-5}[\mathrm{PAPA/NO}] \quad \text{Eq. (5b)}$$

Thus, the observed dependence of V_{max} on PAPA/NO is in agreement with theoretical analysis for both kinetic mechanisms.

Validation of rate law and data fitting

To validate the assumptions in the pseudo steady state approximation, we compared the proposed rate law (Eq. 2b) with the numerical solution of the complete set of ordinary differential equations describing the second kinetic mechanism (Reactions 1, 2, 4, 5, and 6) and assuming values for kinetic constants from Table 1. Rate law and numerical solution provide essentially identical results (data not shown). Thus, Eq. 2b accurately describes the behavior of the second kinetic mechanism.

We further validated the proposed rate laws (Eq. 2b – 2d) against our experimental data and we tested if measured GSNO formation rates are in agreement with predicted rates from the rate laws. Previously determined values for reaction rate constants were assumed (Table 1). Each NO donor concentration was related to the corresponding clamped NO concentration based on Eq. 3. In Fig. 5 rate law predictions are presented as solid lines and experimental data with different symbols for each NO donor (or NO) concentration. Dotted lines depict model simulations of the set of all 25 reactions presented in the Supplement. From the three rate laws, only Eq. 2d is shown. Eq. 2b and 2c yield similar results as 2d over the range of GSH examined, and hence they were omitted from Fig. 5. There is close agreement between rate law, model simulations and experimental data over a wide range of NO and GSH concentrations. There is a difference between rate law and model for high NO indicating that additional reactions that have not been incorporated in the simplified kinetic mechanism become more important as NO concentration increases. The accuracy of the experimental data does not allow confirming this limitation of the rate law at high NO concentrations.

Eq. 2c suggests that when the ratio of [NO] to [GSH] is not much greater than $\frac{k_8 k_7}{k_6 k_7}$ reactions 7–9 become important. Based on previous estimates for constants k_6, k_7, k_{-7}, and k_8 (Table 1) this ratio should be equal to 5×10^{-4}μM NO/μM GSH. In the experimental results presented in Fig. 5, the ratios of [NO]/[GSH] were between 10^{-3}–10^{-1} thus, these reactions should not have affected GSNO formation. In the supplement, we present model simulations for higher GSH concentrations (Fig. S1). GSNO formations rates show a decrease at high [GSH] that cannot be captured by the rate law of Eq. 2b. On the contrary, Eq. 2c is in agreement with model simulations suggesting that this effect is attributed to Reactions 7–9.

Eq. 2d suggests that when $[\mathrm{GSNO}] \ll \frac{k_6}{k_{10}}[\mathrm{NO}]$ Reaction 10 does not affect formation rate. By measuring formation rates within a few seconds after mixing of the reactants we can minimize the effect of this reaction. At longer times, when [GSNO] approaches $\frac{k_6}{k_{10}}[\mathrm{NO}]$, an effect of this reaction can be observed(data not shown). Thus, under our experimental conditions and for the range of NO and GSH concentrations examined Reactions 1, 2, 4, 5, and 6 are the ones that mostly determine GSNO formation rate.

Discussion

Recent evidence for contribution of $^{\bullet}NO_2$ radical in the nitrosation of thiols [8, 16, 22, 39] provided the incentive to revisit an earlier proposed kinetic law by Kharitonov et al. [17] for the nitrosation of thiols. We followed a similar theoretical analysis (i.e. PSSA) with this earlier study for two alternative reaction schemes; one where N_2O_3 is the nitrosating intermediate and one where $^{\bullet}NO_2$ plays this role. Earlier experimental data have confirmed saturation kinetics of the nitrosation rate on GSH concentration [7, 17, 36]. This is in agreement with both kinetic mechanisms. Previous studies however, did not examine if the GSH concentration for half-maximum rate (i.e. EC_{50}) remains constant at different NO

concentration levels. Theoretical analysis suggests that unlike in N_2O_3-based nitrosation, in a primarily $^{\bullet}NO_2$-based nitrosation the EC_{50} will increase as the NO concentration increases.

Experimental findings in this study confirm such dependence and argue for significant contribution of the second kinetic mechanism in GSH nitrosation. Our data show that GSNO formation rate follows saturation kinetics with respect to GSH concentration and EC_{50} increases with NO donor concentration. Data suggests an EC_{50} that is proportional to [NO] (Fig. 3). This is in agreement with $^{\bullet}NO_2$ based nitrosation (Eq. 2b).

Theoretical considerations corroborated by experimental data show that in aerated slow-releasing NO donor solutions, NO levels remain relatively steady with a concentration that increases proportionally to the square root of the NO donor concentration (Fig. 1). This enables us to monitor the reaction over longer periods of time (i.e. no need for rapid mixing in a stop-flow apparatus) and to relate the rate of GSNO formation to the NO concentration. [Caution however is advised since at later times conversion of GSNO to GSSG might influence GSNO formation rate]. We utilized two alternative methods to assess GSNO concentration. With the spectrophotometrical method, GSNO is measured continuously during the reaction, while chemiluminescence requires stopping the reaction at different time points and assess GSNO after a long incubation time to release excess NO from the system. As a result, rates estimated with the second method may have less accuracy.

Goldstein et al [18] has previously suggested that $^{\bullet}NO_2$ can act as an active intermediate for GSH nitrosation. They presented kinetic laws that propose a functional difference between $^{\bullet}NO_2$ and N_2O_3 mechanisms similar to this study (Note: Eq. 21 and 22 in [18] propose similar saturation kinetics but for the nitrosation yield instead of the reaction rate). These two quantities should follow a similar dependence on GSH and NO, at initial times. This functional difference was tested for some thiols (NAPenSH) showing dependence characteristic of the N_2O_3 based pathway. The authors concluded that both $^{\bullet}NO_2$ and N_2O_3 can play the role of active intermediate in thiol nitrosation.

Schrammel et al [8] have provided evidence for $^{\bullet}NO_2$ as the main nitrosating intermediate for GSH and albumin. The nitrosation was partially inhibited in the presence of thiyl scavengers (ascorbate and TEMPOL) and EPR spectroscopy revealed intermediate formation of glutathionyl radicals. They concluded that GSNO formation by NO/O_2 is predominantly mediated by $^{\bullet}NO_2$. However, TEMPOL may not impact solely the thiyl radical since scavenging of $^{\bullet}NO_2$ has also been suggested [41]. This would presumably interfere with the N_2O_3 pathway as well (Reaction 3). Jourd'heuil et al. [39] have also provided evidence for $^{\bullet}NO_2$ over N_2O_3 as the nitrosating intermediate. Inhibition of thiyl radical-mediated GSNO and GSSG formation by the thiyl radical trap 5,5-dimethyl-1-pyrroline N-oxide (DMPO) was demonstrated. However, nitrosation was shown to be insensitive to DMPO in an earlier study [40]. Thus, although the recent use of spin traps has provided evidence for a significant role of $^{\bullet}NO_2$ in thiol nitrosation, the relative importance of the two alternative intermediates remains a topic of continuing investigations. A recent study by Keszler et al [22] utilizes theoretical analysis and experimentation and suggests involvement of both intermediates in nitrosation. Simplified rate laws were provided for N_2O_3 but not for $^{\bullet}NO_2$ nitrosation. A detailed kinetic model that includes 20 relevant reactions was proposed and was fitted to the experimental data. Evidence for N_2O_3 contribution is provided by the reported decrease in GSNO formation when N_2O_3 hydrolysis is enhanced. A 10-fold increase in the rate of N_2O_3 mediated nitrosation (Reaction 3) than previously reported was actually suggested to explain a decrease in GSSG with a concomitant increase in GSNO when a thiyl radical trap (DMPO) was utilized. This allows for significant increase in GSNO formation through mechanism 1(N_2O_3 based nitrosation scheme) when mechanism 2 ($^{\bullet}NO_2$ based nitrosation scheme) is inhibited. Thus, there is

conflicting evidence for the effect of thiyl radical scavenging on GSNO formation with some studies reporting a decrease [8, 39] while others an increase [22, 65]. However, as pointed outin [22], cross talk between the two pathways makes difficult the interpretation of the results and to conclusively determine which is the dominant mechanism.

There is a good agreement between our estimated kinetic constant for thiol oxidation by $^{\bullet}NO_2$ (i.e. $k_5 = 1.15\times10^7\ M^{-1}s^{-1}$) and the constant provided by Ford et al. [31] (i.e $1\times10^7\ M^{-1}s^{-1}$ and $2\times10^7\ M^{-1}s^{-1}$ after correction for a side reaction). Based on this value the authors in this earlier study argued, that there is small likelihood for significant generation of N_2O_3 (Reaction 2) compared to the loss of $^{\bullet}NO_2$ via reaction such as Reaction 5, and thus, a substantial fraction of any $^{\bullet}NO_2$ produced should not be channeled to nitrosative chemistry involving N_2O_3. This suggests a dominant role of $^{\bullet}NO_2$ in nitrosation of thiols and a lesser role for N_2O_3. Our theoretical analysis demonstrates this point in a system containing a significant number of the most relevant reactions.

An important observation in previous studies [22, 39, 40, 65] is the significant generation of GSSG. Reactants and active intermediates may be utilized for the generation of GSSG and this utilization can affect GSNO formation rate. This represents a serious threat for the accuracy of the proposed simplified rate laws (Eq. 2a and Eq. 2b) presented here or in previous studies. The reaction scheme presented in the supplement proposes four alternative pathways for GSSG formation (Reactions 8, 10, 11, 18) out of which Reactions 8 and 10 are the most important based on the assumed values for the kinetic constants. Interestingly, Reaction 8 becomes important for low [NO]/[GSH] ratios while Reaction 10 is important after significant GSNO accumulations and thus high [GSNO]/[NO] ratios. Thus, the proposed rate law in Eq. 2b can adequately describe our data since the high [NO]/[GSH] ratio and the estimation of GSNO formation rate early (i.e. low [GSNO]/[NO] ratio) should provide conditions for low GSSG formation rate. [Note that previous studies [22, 39, 40, 65] have often used lower [NO]/[GSH] ratios and reaction is followed for several minutes]. Interference from Reaction 8 will occur at low [NO]/[GSH] ratios and will be documented with a decrease in GSNO formation rate as GSH concentration increases (Fig. S1). Interference from Reaction 10 will appear after significant GSNO accumulation and will be documented with a saturation of GSNO concentration with time. In this study, the nitrosation mechanism was tested only for glutathione. Previous studies have shown similar kinetic behavior in the nitrosation of Cysteine, whereas for other thiols like N-acetyl Penicillamine (NAPenSH), captopril (CapSH) and N-nitrosomorpholine (MorNNO) the oxidizing reaction through $^{\bullet}NO_2$ has been found to be too slow and Reaction 2 was found to outcompete their oxidation by $^{\bullet}NO_2$ [18].

In vivo, the nitrosation pathway could be affected by the slow NO oxidation and other reaction pathways could become important. It has been previously suggested [16, 19, 20, 21, 25, 28], that catalysis of nitric oxide oxidation in hydrophobic environments is possible which might accelerate formation rate. The physiological relevance of the nitrosation process and the ability of thiols to transport and preserve NO might hinge on acceleration of nitrosation in hydrophobic environments (owing to $< 1\ \mu M$ [NO] in vivo and the slow NO oxidation process in aqueous solution), and thus this needs further study. In addition, the effects of transition metal ions [27], cellular antioxidants [29] and lipid radical species [30]and pH variations [31] need to be further examined. There is also a possibility of a heme enzyme dependent nitrosation[67]. Glutathione may bind to ferric cytochrome c followed by a combination of NO to form a ferric cyt-c GSNOH complex. Subsequent electron donation from NO to heme would then, yield ferrous cytochrome c and GSNO. Experimental evidence with isolated enzymes and in cells corroborate this hypothesis [68]. Besides cytochrome c, other heme enzymes and iron complexes may serve similar functions [69, 70, 71, 72].

In summary, recent studies point towards a role of $^{\bullet}NO_2$ in thiol nitrosation. However, the relative contribution of N_2O_3 and $^{\bullet}NO_2$ has been difficult to elucidate so far, as a result of cross talk between the two alternative mechanisms. In this study, theoretical analysis suggests a functional difference in the rate laws between N_2O_3 and $^{\bullet}NO_2$ mediated nitrosation (Eq. 2a and 2b) and experimental data suggest a predominant role for $^{\bullet}NO_2$ in the nitrosation of GSH by NO donors in aerated solutions. In vivo, a series of factors may interfere with the nitrosation pathway and the relative importance of the two intermediates needs to be further investigated.

Supplementary Material

Refer to Web version on PubMed Central for supplementary material.

Acknowledgments

This work was funded by National Institutes of Health Grant SC1HL095101 (NT).

References

1. Ignarro LJ, Buga GM, Wood KS, Byrns RE. Endothelial-derived relaxing factor produced and released from artery and vein is nitric oxide. Proc Natl Acad Sci USA. 1987; 84:9265–9269. [PubMed: 2827174]
2. Bredt DS, Snyder SH. Nitric oxide mediates glutamate- linked enhancement of cGMP levels in the cerebellum. Proc Natl Acad Sci USA. 1989; 86:9030–9033. [PubMed: 2573074]
3. Stuehr DJ, Marletta MA. Mammalian nitrate biosynthesis: Mouse macrophages produce nitrite and nitrate in response to Escherichia coli lipopolysaccharide. Proc Natl Acad Sci USA. 1985; 82:7738–7742. [PubMed: 3906650]
4. Lancaster JR Jr. Simulation of the diffusion and reaction of endogenously produced nitric oxide. Proc Natl Acad Sci USA. 1994; 91:8137–8141. [PubMed: 8058769]
5. Jia L, Bonaventura C, Bonaventura J, Stamler JS. S-nitrosohaemoglobin: a dynamic activity of blood involved in vascular control. Nature. 1996; 380:221–226. [PubMed: 8637569]
6. Ignarro LJ, Lipton H, Edwards JC, Baricos WH, Hyman AL, Kadowitz PJ, Gruetter CA. Mechanism of vascular smooth muscle cell relaxation by organic nitrates, nitrites, nitroprusside and nitric oxide: Evidence for the involvement of S-nitrosothiols as active intermediates. J Pharmacol Exp Ther. 1981; 218:739–749. [PubMed: 6115052]
7. Wink DA, Darbyshire JF, Nims RW, Saavedra JE, Ford PC. Reactions of the bioregulatory agent nitric oxide in oxygenated aqueous media: determination of the kinetics for oxidation and nitrosation by intermediates generated in the NO/O2 reaction. Chem Res Toxicol. 1993; 6(1):23–27. [PubMed: 8448345]
8. Schrammel A, Gorren ACF, Schmidt K, Pfeiffer S, Mayer B. S-Nitrosation of Glutathione by Nitric Oxide, Peroxynitrite and NO/O_2. Free Radic Biol Med. 2003; 34(8):1078–1088. [PubMed: 12684093]
9. Field L, Dilts RV, Ravichandran R, Lenhert PG, Carnahan GF. An Unusually Stable Thionitrite from N-Acetyl-D, L-penicillamine; X-Ray Crystal and Molecular Structure of 2-(Acetylamino)-2-carboxy-1,1-dimethylethyl Thionitrite. J Chem Soc Chem Commun. 1978; 6:249–250.
10. Williams DLH. S-Nitrosothiols and role of metal ions in decomposition to nitric oxide. Methods Enzymol. 1996; 268:299–308. [PubMed: 8782596]
11. Fang K, Ragsdale NV, Carey RM, MacDonald T, Gaston B. Reductive Assays for S-Nitrosothiols: Implications for Measurements in Biological Systems. Biochem Biophys Res Commun. 1998; 252(3):535–540. [PubMed: 9837741]
12. Gorren AC, Schrammel A, Schmidt K, Mayer B. Decomposition of S-nitrosoglutathione in the presence of copper ions and glutathione. Arch Biochem Biophys Arch Biochem Biophys. 1996; 330(2):219–28.

13. Saville B. A scheme for the colorimetric determination of microgram amounts of thiols. Analyst. 1958; 83:670–672.
14. Keefer LK, Nims RW, Davies KM, Wink DA. “NONOates” (1-substituted diazen-1-ium-1,2-diolates) as nitric oxide donors: convenient nitric oxide dosage forms. Methods Enzymol. 1996; 268:281–293. [PubMed: 8782594]
15. Maragos CM, Morley D, Wink DA, Dunams TM, Saavedra JE, Hoffman A, Bove A, Isaac L, Hrabie JA, Keefer LK. Complexes of NO with Nucleophiles as agents for the Controlled Biological Release of Nitric Oxide Vasorelaxant effects. J Med Chem. 1991; 34:3242–3247. [PubMed: 1956043]
16. Nedospasov AA. Is N_2O_3 the main nitrosating intermediate in aerated nitric oxide (NO) solutions in vivo? If so, where, when, and which one? J Biochem Mol Toxicol. 2002; 16(3):109–120. [PubMed: 12112710]
17. Kharitonov VG, Sundquist AR, Sharma VS. Kinetics of nitrosation of thiols by nitric oxide in the presence of oxygen. J Biol Chem. 1995; 269:28518–28164.
18. Goldstein S, Czapski G. Mechanism of the nitrosation of thiols and amines by oxygenated radical NO solutions, the nature of the nitrosating intermediates. J Am Chem Soc. 1996; 118:3419–3425.
19. Gordin VA, Nedospasov AA. NO catastrophes in vivo as a result of micellar catalysis. FEBS Lett. 1998; 424:239–242. [PubMed: 9539158]
20. Nedospasov AA. Competition involving biogenic NO. Biochemistry (Moscow). 1998; 63:744–765. [PubMed: 9721328]
21. Liu X, Miller MJS, Joshi MS, Thomas DD, Lancaster JR Jr. Accelerated reaction of nitric oxide with O_2 within the hydrophobic interior of biological membranes. Proc Natl Acad Sci USA. 1998; 95:2175–2179. [PubMed: 9482858]
22. Keszler A, Zhang Y, Hogg N. The reaction between nitric oxide, glutathione and oxygen in the presence and absence of protein: How are S-nitrosothiol formed? Free Radic Biol Med. 2010; 48(1):55–64. [PubMed: 19819329]
23. Gow AJ, Buerk DG, Ischiropoulos H. A novel reaction mechanism for the formation of S – nitrosothiol in vivo. J Biol Chem. 1997; 272:2841–2845. [PubMed: 9006926]
24. Samouilov A, Zweier JL. Development of chemiluminescence based methods for specific quantitation of nitrosylated thiols. Anal Biochem. 1998; 258:322–330. [PubMed: 9570848]
25. Rafikova O, Rafikov R, Nudler E. Catalysis of S-nitrosothiols formation by serum albumin: the mechanism and implication in vascular control. Proc Natl Acad Sci USA. 2002; 99:5913–5918. [PubMed: 11983891]
26. Lancaster JR. Nitroxidative, Nitrosative, and Nitrative Stress: Kinetic Predictions of Reactive Species Chemistry Under Biological Conditions. Chem Res Toxicol. 2006; 19:1160–1174. [PubMed: 16978020]
27. Thomas DD, Miranda KM, Colton CA, Citrin D, Espey MG, Wink DA. Heme proteins and nitric oxide (NO): the neglected eloquent chemistry in NO redox signaling and regulation. Antioxid Redox Signaling. 2003; 5:307–317.
28. Goss SP, Singh RJ, Hogg N, Kalyanaraman B. Reactions of $^{*}NO$, $^{*}NO_2$ and peroxynitrite in membranes: physiological implications. Free Radical Res. 1999; 31:597–606. [PubMed: 10630683]
29. Hooper DC, Spitsin S, Kean RB, Chapion JM, Dickson GM, Chaudry I. Uric acid, a natural scavenger of peroxynitrite, in experimental allergic encephalomyelitis and multiple sclerosis. Proc Natl Acad Sci USA. 1998; 95:675–680. [PubMed: 9435251]
30. Rubbo H, Parthasarathy S, Barnes S, Kirk M, Kalyanaraman B, Freeman BA. Nitric oxide inhibition of lipoxygenase- dependent liposome and low density lipoprotein oxidation: termination of radical chain propagation reactions and formation of nitrogen containing oxidized lipid derivatives. Arch Biochem Biophys. 1995; 324:15–25. [PubMed: 7503550]
31. Ford E, Hughes MN, Wardman P. Kinetics of the Reactions of Nitrogen Dioxide with Glutathione, Cysteine and Uric Acid at Physiological pH. Free Radic Biol Med. 2002; 32:1314–1323. [PubMed: 12057769]
32. Coddington JW, Hurst JK, Lymar SV. Hydroxyl radical formation during peroxynitrous acid decomposition. J Am Chem Soc. 1999; 121:2438–2443.

33. Keshive M, Singh S, Wishnok JS, Tannenbaum SR, Deen WM. Kinetics of S –nitrosation of Thiols in nitric oxide solutions. Chem Res Toxicol. 1996; 9:988–993. [PubMed: 8870986]
34. Goldstein S, Czapski G. Reactivity of peroxynitrite versus simultaneous generation of NO and O_2^- toward NADH. Chem Res Toxicol. 2000; 13:736–741. [PubMed: 10956061]
35. Merenyi G, Lind J, Goldstein S, Czapski G. Mechanism and thermochemistry of peroxynitrite decomposition. J Phys Chem. 1999; 103:5685–5691.
36. Wink DA, Nims RW, Darbyshire JF, Christodoulou D, Hanbauer I, Cox GW, Laval F, Laval J, Cook JA, Krishna MC, DeGraff WG, Mitchell JB. Reaction Kinetics for Nitrosation of Cysteine and Glutathione in Aerobic Nitric Oxide Solutions at Neutral pH. Insights into the Fate and Physiological Effects of Intermediates Generated in the NO/O_2 Reaction. Chem Res Toxicol. 1994; 7:519–525. [PubMed: 7981416]
37. Kissner R, Nauser T, Bugnon P, Lye PG, Koppenol WH. Formation and properties of peroxynitrite as studied by laser flash photolysis, high pressure stopped flow technique and pulse radiolysis. Chem Res Toxicol. 10:1285–1292. [PubMed: 9403183]
38. Meister A, Anderson ME. Glutathione. Annu Rev Biochem. 1983; 52:711–760. [PubMed: 6137189]
39. Jourd'heuil D, Jourd'heuil FL, Feelisch M. Oxidation and nitrosation of thiols at low micromolar exposure to nitric oxide. Evidence for a free radical mechanism. J Biol Chem. 2003; 278(18): 15720–15726. [PubMed: 12595536]
40. Hogg N, Singh RJ, Kalyanaraman B. The role of glutathione in the transport and catabolism of nitric oxide. FEBS Lett. 1996; 82(3):223–228. [PubMed: 8605974]
41. Carroll RT, Galatsis P, Borosky S, Kopec KK, Kumar V, Althaus JS, Hall ED. 4-Hydroxy-2,2,6,6,-tetramethylpiperidine-1-oxyl (Tempol) inhibits peroxynitrite mediated phenol nitration. Chem Res Toxicol. 2000; 13:294–300. [PubMed: 10775330]
42. Lim CH, Dedon PC, Deen WM. Kinetic Analysis of Intracellular Concentrations of Reactive Nitrogen Species. Chem Res Toxicol. 2008; 21:2134–2147. [PubMed: 18828639]
43. Tamba M, Simone G, Quintiliani M. Interactions of thiyl free radicals with oxygen: a pulse radiolysis study. Int J Radiat Biol. 1986; 50:595–600.
44. Goldstein S, Czapski G. Kinetics of Nitric Oxide Autoxidation in Aqueous Solution in the Absence and Presence of Various Reductants. The Nature of the Oxidized Intermediates. J Am Chem Soc. 1995; 117:12078–12084.
45. Schwartz, SE. Advances in Environmental Science and Technology. New York: Wiley; 1969. Trace atmospheric constituents: Properties, transformations and fates; p. 1-115.
46. Wardman P. Evaluation of the "radical sink" hypothesis from a chemical-kinetic view point. J Radioanal Nucl Chem. 1998; 232:23–27.
47. Wardman P, von Sontag C. Kinetic Factors that Control the Fate of Thiyl Radicals in Cells. Methods Enzymol Methods Enzymol. 1995; 251:31–45.
48. Hoffman MZ, Hayon E. Pulseradiolysis Study of Sulfhydryl Compounds in Aqueous Solution. J Phys Chem. 1973; 77:990–996.
49. Kirsch M, Lehnig M, Korth HG, Sustmann R, de Groot H. Inhibition of Peroxynitrite Induced Nitration of Tyrosine by Glutathione in the Presence of Carbon Dioxide through both Radical Repair and Peroxynitrate Formation. Eur Chem J. 2001; 7:3313–3320.
50. Wood PD, Mutus B, Redmond RW. The Mechanism of Photochemical Release of Nitric Oxide from S-Nitrosoglutathione. Photochem Photobiol. 1996; 64:518–524.
51. Bonini MG, Augusto O. Carbon dioxide stimulates the production of thiyl, sulfinyl and disulfide radical anion from thiol oxidation by peroxynitrite. J Biol Chem. 2001; 276:9749–9754. [PubMed: 11134018]
52. Jourd'heuil D, Jourd'heuil FL, Kutchukian PS, Musah RA, Wink DA, Grisham MB. Reaction of superoxide and nitric oxide with peroxynitrite. Implications for peroxynitrite-mediated oxidation reactions in vivo. J Biol Chem. 2001; 276:28799–28805. [PubMed: 11373284]
53. Santos C, Bonini MG, Augusto O. Role of the carbonate anion in tyrosine nitration and hydroxylation by peroxynitrite. Arch Biochem Biophys. 2000; 77:146–152. [PubMed: 10775454]

54. Ross, AB.; Mallard, WG.; Helman, WP.; Buxton, GV.; Hurie, RE.; Neta, P. NDRL/NIST Solution Kinetics Database, version 3. Notre Dame Radiation Laboratory; Gaithersburg, MD: 1998. http://www.rcdc.nd.edu/browse_compil.html
55. Behar D, Czapski G, Rabani J, Dirman LM, Schwarz HA. The Acid Dissociation Constant and Decay Kinetics of the Perhydroxyl Radical. J Phys Chem. 1970; 74:3209–3213.
56. Broszkiewicz RK. The pulse radiolysis study of $NaNO_2$ and $NaNO_3$ solutions. Bull Acad Pol Sci Sedr Sci Chim. 1976; 24:221–229.
57. Schwartz SE, White WH. Kinetics of reactive dissolution of nitrogen oxide in aqueous solution. Adv Environ Sci Technol. 1983; 12:1–116.
58. Czapski G, Goldstein S. The role of the reactions of NO with superoxide and oxygen in biological systems: A kinetic approach. Free Radic Biol Med. 1995; 19:785–794. [PubMed: 8582651]
59. Griffiths C, Wykes V, Bellamy TC, Garthwaite J. A new and simple method for delivering clamped nitric oxide concentrations in the physiological range: application to activation of guanylyl cyclase coupled nitric oxide receptors. Mol Pharmacol. 2003; 64(6):1349–56. [PubMed: 14645665]
60. Thomas DD, Miranda KM, Espey MG, Citrin D, Jourd'heuil D, Paolocci N, Hewett SJ, Colton CA, Grisham MB, Feelisch M, Wink DA. Guide for the use of nitric oxide (NO) donors as probes of the chemistry of NO and related redox species in biological systems. Methods Enzymol. 2002; 359:84–105. [PubMed: 12481562]
61. Li Q, Lancaster JR Jr. Calibration of nitric oxide flux generation from diazeniumdiolate *NO donors. Nitric Oxide. 2009; 21(1):69–75. [PubMed: 19366637]
62. Kharitonov VG, Sundquist AR, Sharma VS. Kinetics of nitric oxide autoxidation in aqueous solution. J Biol Chem. 1994; 269(8):5881–5883. [PubMed: 8119931]
63. Goldstein S, Russo A, Samuni A. Reactions of PTIO and Carboxy-PTIO with NO, NO_2 and O_2. J Biol Chem. 2003; 278:50949–50955. [PubMed: 12954619]
64. Luo D, Smith SW, Anderson BD. Kinetics and mechanism of the reaction of cysteine and hydrogen peroxide in aqueous solution. J Pharm Sci. 2005; 94:304–316. [PubMed: 15570599]
65. Koshiishi I, Takajo T, Tsuchida K. Regulation of S-thiolation and S-nitrosylation in the thiol/nitric oxide system by radical scavengers. Nitric Oxide. 2007; 16:356–361. [PubMed: 17293136]
66. Madej E, Folkes LK, Wardman P, Czapski G, Goldstein S. Thiyl radicals react with nitric oxide to form S-nitrosothiols with rate constants near the diffusion controlled limit. Free Radic Biol Med. 2008; 44:2013–2018. [PubMed: 18381080]
67. Basu S, Keszler A, Azarova NA, Nwanze N, Perlegas A, Shiva S, Broniowska KA, Hogg N, Kim–Shapiro DB. A novel role for cytochrome c: Efficient catalysis of S-nitrosothiol formation. Free Radic Biol Med. 2010; 48:255–263. [PubMed: 19879353]
68. Broniowska KA, Keszler A, Basu S, Kim-Shapiro DB, Hogg N. Cytochrome c-mediated formation of S-nitrosothiol in cells. Biochem J. 2012; 441:191–197. [PubMed: 22070099]
69. Bosworth CA, Toledo JC, Zmijewski JW, Li Q, Lancaster JR. Dinitrosyliron complexes and the mechanism(s) of cellular protein nitrosothiol formation from nitric oxide. Proc Natl Acad Sci. 2009; 106(12):4671–4676. [PubMed: 19261856]
70. Inoue K, Akaike T, Miyamoto Y, Okamoto T, Sawa T, Otaqiri M, Suzuki S, Yoshimura T, Maeda H. Nitrosothiol formation catalyzed by ceruloplasmin. Implication for cytoprotective mechanism in vivo. J Biol Chem. 1999; 274(38):27069–27075. [PubMed: 10480920]
71. Weischel A, Maes EM, Andersen JF, Valenzuela JG, Shokhireva TKh, Walker FA, Montfort WR. Heme-assisted S-nitrosation of a proximal thiolate in a nitric oxide transport protein. Proc Natl Acad Sci USA. 2005; 102(3):594–599. [PubMed: 15637157]
72. Luchsinger BP, Rich EN, Gow AJ, Williams EM, Stamler JS, Singel DJ. Routes to S-nitroso-hemoglobin formation with heme redox and preferential reactivity in the beta subunits. Proc Natl Acad Sci USA. 2003; 100(2):461–466. [PubMed: 12524454]
73. Gaston B, Sears S, Woods J, Hunt J, Ponaman M, McMahon T, Stamler JS. Bronchodilator S-nitrosothiol deficiency in asthmatic respiratory failure. Lancet. 1998; 351:1317–1319. [PubMed: 9643794]

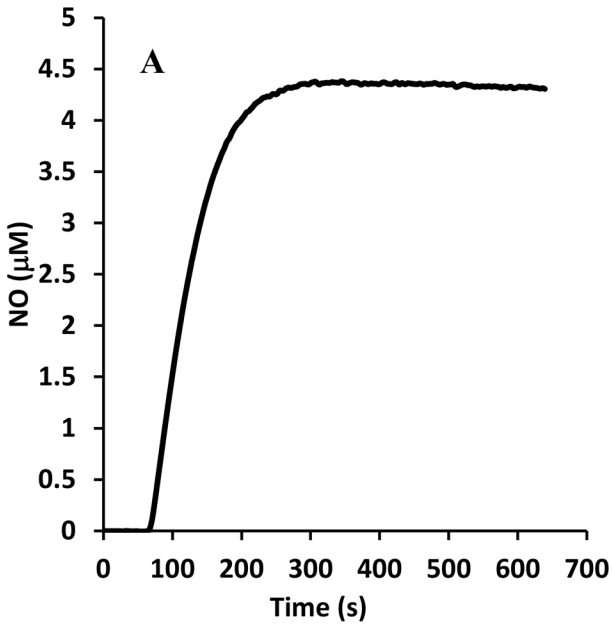

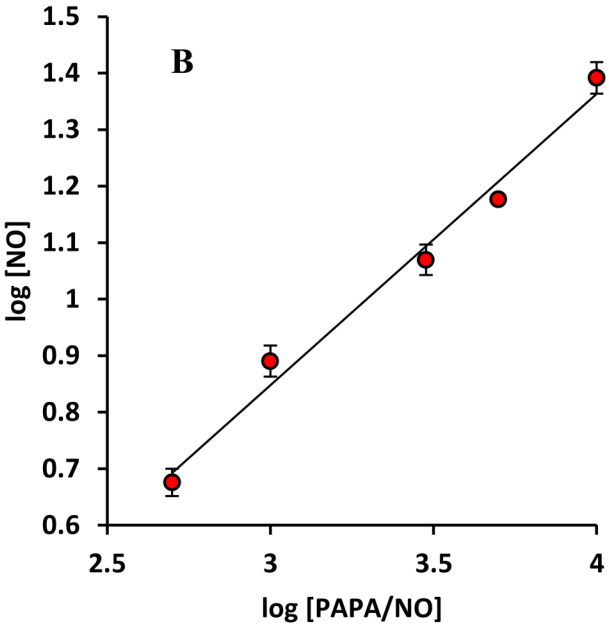

FIGURE 1.

(A) Release of NO from PAPA/NO (500 μM). NO concentration is monitored with a NO-sensitive electrode for 30 min. After an initial accumulation period, NO levels remain relative steady for a significant time period. (B) log-log graph showing relation between maximum NO concentrations achieved at different PAPA/NO concentrations (n = 4). The slope of 0.51 ± 0.04 is not statistically different from 0.5 ($p = 0.30$).

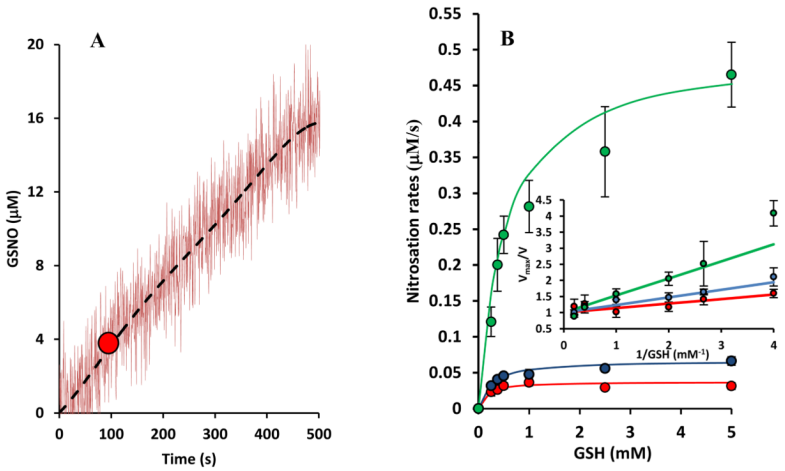

FIGURE 2.

(A) Representative data for GSNO formation as a function of time. GSNO concentration was monitored in a spectrophotometer at 338 nm, following mixing of GSH (250 μM) and PAPA/NO (1 mM). Data were fitted by a 5th order polynomial to remove noise (dashed black line). The maximum slope of the polynomial is identified (red circle) and corresponds to the GSNO formation rate at peak NO concentration. (B) Rates of nitrosation (V) at three different NO donor concentrations (500 μM (red), 1 mM (blue) and 5 mM (green)) are plotted against GSH concentrations. Inset shows V_{max}/V plotted against 1/GSH. Slope of these lines indicate EC_{50} values. An increase in EC_{50} values is observed with increasing NO donor concentrations.

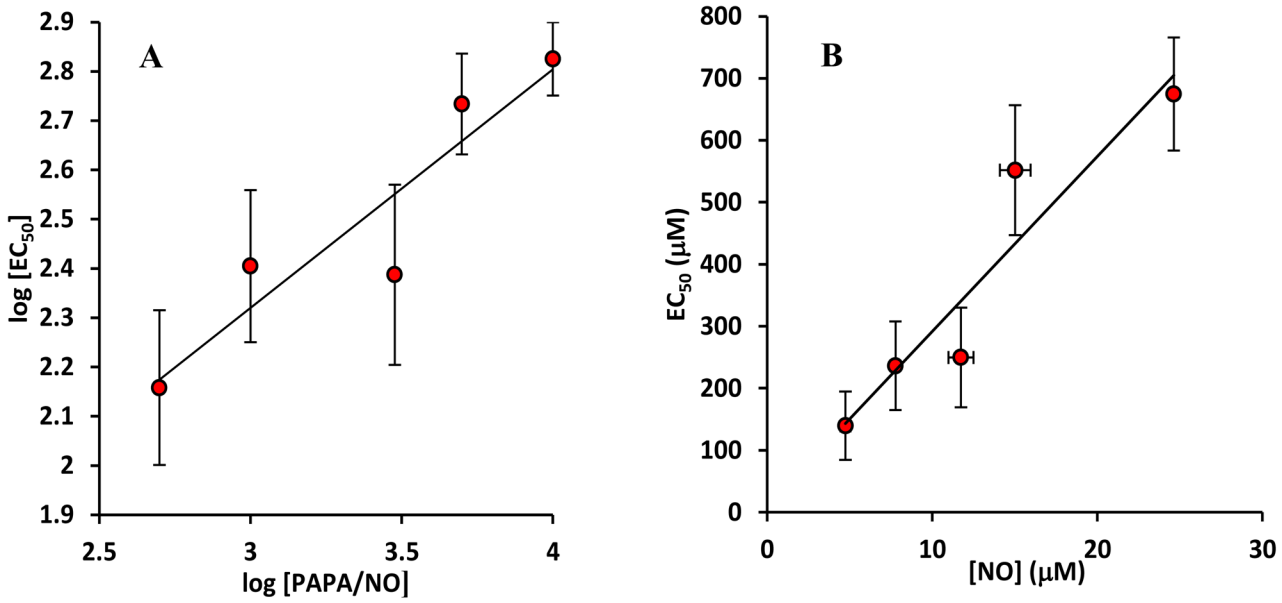

FIGURE 3.

(A) A log – log graph of half maximum constant (EC_{50}) at different PAPA/NO concentrations. Average EC_{50} values (n = 3) are presented. The slope of 0.5 ± 0.2 is not statistically different from 0.5 (p = 0.946). The result suggests that EC_{50} is proportional to the square root of NO donor concentration and thus proportional to NO concentration. (B) A graph of EC_{50} vs. clamped NO values from NO electrode measurements in Fig 1B. The slope from a linear fit of the graph is 30.5 ± 5.2 μM GSH/μM.

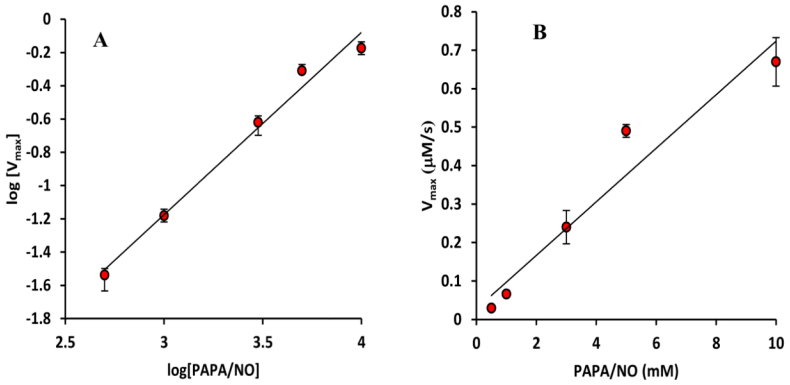

FIGURE 4.

(A) A log – log graph of nitrosation rates at saturating GSH concentrations (V_{max}) at different PAPA/NO concentrations. Average values with standard deviations (error bars) are presented. A linear fit gives a slope of 1.08 ± 0.1. The slope is not statistically different from 1 ($p = 0.09$) and significantly different from 0.5 and 1.5 ($p \ll 0.05$) suggesting a V_{max} proportional to the NO donor concentration. (B) The linear dependence of V_{max} on PAPA/NO concentration has a slope of $(7.5 \pm 0.5) \times 10^{-5}\ s^{-1}$.

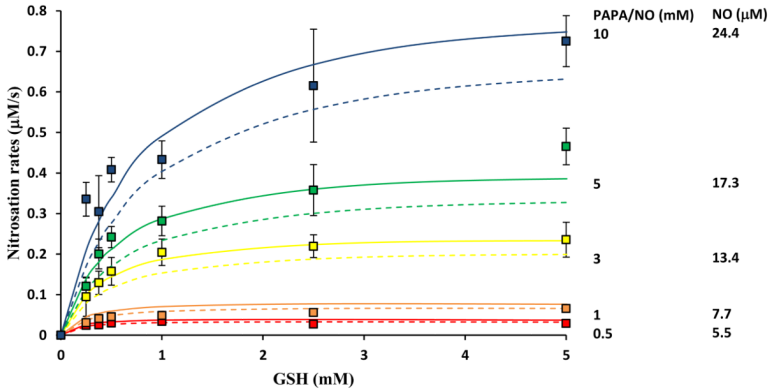

FIGURE 5.

Comparison of GSNO formation rates as predicted by the proposed rate law of the simplified reaction scheme Eq. 2d (solid lines), the mathematical model of the complete reaction set (dotted lines) next to experimental data. Data using different PAPA/NO concentrations are presented (500 μM, 1 mM, 3 mM, 5 mM and 10 mM). The corresponding NO concentration achieved were. Error bars show standard deviations (n = 3).

Table T1

Rate constants of reactions mentioned in the manuscript are as follows:

Reaction No.	Reaction	Rate constant	Reference
1	$2NO+O_2 \xrightarrow{k_1} 2NO_2$	$k_1 = 2.9\times10^6\ M^{-2}s^{-1}$	[44, 58]
2	$NO+NO_2 \underset{k_{-2}}{\overset{k_2}{\rightleftharpoons}} N_2O_3$	$k_2 = 1.1\times10^9\ M^{-1}s^{-1}$ $k_{-2} = 8.1\times10^4\ s^{-1}$	[18] [18]
3	$N_2O_3+GSH \xrightarrow{k_3} GSNO+NO_2^-+H^+$	$k_3 = 6.6\times10^7\ M^{-1}s^{-1}$	[33]
4	$N_2O_3+H_2O \xrightarrow{k_4} 2NO_2^-+2H^+$	$k_4 = 3.8\times10^4\ s^{-1}$	[18]
5	$^{\cdot}NO_2+GSH \xrightarrow{k_5'} NO_2^-+GS^{\cdot}+H^+$ $^{\cdot}NO_2+GS^- \xrightarrow{k_5''} NO_2^-+GS^{\cdot}$	$k_5 = 1.15\times10^7\ M^{-1}s^{-1}$ $\left(k_5=k_5'+k_5''\frac{[GS^-]}{[GSH]}\right)$	Estimated See also [31]
6	$GS^{\cdot}+^{\cdot}NO \xrightarrow{k_6} GSNO$	$k_6 = 3\times10^9\ M^{-1}s^{-1}$	[66]
7	$GSH \underset{k_{-7}}{\overset{k_7}{\rightleftharpoons}} GS^-+H^+$	$k_7 = 63\ s^{-1}$ $k_{-7} = 0.1\times10^{10}\ M^{-1}s^{-1}$	[46] [46]*
8	$GS^{\cdot}+GS^- \underset{k_{-8}}{\overset{k_8}{\rightleftharpoons}} GSSG^-$	$k_8 = 9.6\times10^6\ M^{-1}s^{-1}$ $k_{-8} = 1.6\times10^5\ s^{-1}$	[26] [47]
9	$GSSG^-+O_2 \xrightarrow{k_9} GSSG+O_2^{\cdot-}$	$k_9 = 5\times10^9\ M^{-1}s^{-1}$	[47]
10	$GS^{\cdot}+GSNO \xrightarrow{k_{10}} GSSG+^{\cdot}NO$	$k_{10} = 1.7\times10^9 M^{-1}s^{-1}$	[50]

* pH = 7.4